We foresee extension of these spectroscopic probes to other formally electron-deficient monomers to assess the extent of ligand π donation in organometallic compounds. Control of LUMO properties through ligand π donation has important implications for unsaturated intermediates as well as for formal 16-electron complexes which can be isolated.[27]

Acknowledgment. We wish to thank Professor T. J. Meyer for his constructive scientific suggestions and also for his generosity in providing equipment for the electrochemical measurements. We are grateful to C. R. Leidner for helpful discussions concerning the electrochemical studies. We thank the donors the Petroleum Research Fund, administered by the American Chemical Society, and the NSF (CHE-8310121) for financial support.

(27) Herrick, R. S.; Leazer, D. M.; Templeton, J. L. *Organometallics* **1983**, *2*, 834.

Registry No. $Mo(CO)(MeO_2CC{\equiv}CCO_2Me)(detc)_2$, 56954-20-2; $Mo(CO)(Me_3SiC{\equiv}CSiMe_3)(detc)_2$, 88303-34-8; $Mo(CO)(PhC{\equiv}CPh)(detc)_2$, 56954-16-6; $Mo(CO)(PhC{\equiv}CH)(detc)_2$, 56954-17-7; $Mo(CO)(HC{\equiv}CH)(detc)_2$, 56954-15-5; $Mo(CO)(ClCH_2C{\equiv}CH)(detc)_2$, 88303-35-9; $Mo(CO)(EtC{\equiv}CEt)(detc)_2$, 88303-36-0; $Mo(CO)(MeC{\equiv}CMe)(detc)_2$, 88303-37-1; $Mo(CO)(EtOC{\equiv}CH)(detc)_2$, 88303-38-2; $Mo(CO)(Et_2NC{\equiv}CMe)(detc)_2$, 88303-39-3; $W(CO)(MeO_2CC{\equiv}CCO_2Me)(detc)_2$, 88303-40-6; $W(CO)(Ph_2PC{\equiv}CPPh_2)(detc)_2$, 73848-25-6; $W(CO)(PhC{\equiv}CPh)(detc)_2$, 73848-23-4; $W(CO)(HC{\equiv}CH)(detc)_2$, 66060-14-8; $W(CO)(PhC{\equiv}CH)(detc)_2$, 73848-24-5; $W(CO)(HOCH_2C{\equiv}CCH_2O)(detc)_2$, 88303-41-7; $W(CO)(EtC{\equiv}CEt)(detc)_2$, 73848-22-3; $W(CO)(MeC{\equiv}CMe)(detc)_2$, 73856-95-8; $W(CO)(EtOC{\equiv}CH)(detc)_2$, 88303-42-8; $W(CO)(Et_2NC{\equiv}CMe)(detc)_2$, 88303-43-9; $Mo(MeO_2CC{\equiv}CCO_2Me)_2(detc)_2$, 81476-43-9; $Mo(PhC{\equiv}CPh)_2(detc)_2$, 81476-36-0; $Mo(PhC{\equiv}CMe)_2(detc)_2$, 81476-38-2; $Mo(PhC{\equiv}CH)_2(detc)_2$, 74456-80-7; $Mo(n\text{-}BuC{\equiv}CH)_2(detc)_2$, 81476-41-7; $Mo(EtC{\equiv}CEt)_2(detc)_2$, 81476-40-6; $Mo(CO)_3(detc)_2$, 18866-21-2; $W(CO)_3(detc)_2$, 72827-54-4.

Study of Substituent Effects, Isomerization and Cross Redox Reactions Associated with Electrochemical Oxidation of $Mo(CO)_3P_3$ Systems

A. M. Bond,*[1] S. W. Carr,[2] and R. Colton[2]

Division of Chemical and Physical Sciences, Deakin University, Waurn Ponds, Victoria, 3217, Australia, and the Department of Inorganic Chemistry, University of Melbourne, Parkville, Victoria, 3052, Australia

Received August 10, 1983

Homogeneous and heterogeneous aspects of the redox couple $[Mo(CO)_3P_3]^{+/0}$ (P = monodentate phosphorus ligand) have been examined by polarographic, voltammetric, and spectroscopic methods in dichloromethane solution. The tricarbonyl compounds in each oxidation state can exist in both facial (*fac*$^+$, *fac*^{0}) and meridional (*mer*$^+$, *mer*^{0}) forms. The cyclic voltammograms at room temperature often showed the form of quasi-reversible couples; however, they did not fit theoretical models for simple electron transfer. With use of low temperatures and a variety of scan rates, it was deduced that the electrode processes could be explained in terms of parts of the square reaction scheme

$$\begin{array}{ccc} fac^0 & \rightleftharpoons & fac^+ + e^- \\ \downarrow\uparrow & & \downarrow\uparrow \\ mer^0 & \rightleftharpoons & mer^+ + e^- \end{array}$$

and the cross redox reaction.

$$fac^+ + mer^0 \overset{K}{\rightleftharpoons} fac^0 + mer^+$$

At low temperatures it was possible to calculate $E^\circ(fac^{+/0})$ and $E^\circ(mer^{+/0})$ and hence calculate the equilibrium constant, K, for the cross redox reaction. Both K and the E° values showed a very large dependence on the nature of the phosphorus ligand. For *fac*-$Mo(CO)_3P_3$, a satisfactory linear correlation between carbon-13 NMR chemical shift ($\delta(^{13}C)$) of the carbonyl ligands and $E^\circ(fac^{+/0})$ was obtained, but similar correlations were not observed between $E^\circ(fac^{+/0})$ and either $\delta(^{31}P)$ of the phosphorus ligands or $\delta(^{95}Mo)$ of the central molybdenum atom.

Introduction

Recently there has been considerable interest in the oxidation of 18-electron carbonyl compounds to the 17-electron configuration. A substantial theoretical effort has been made to attempt to understand the effect of the number of carbonyl groups, the influence of the other ligands, the geometry of the complexes, and any structural differences between the 18- and 17-electron states.

A number of workers have attempted to provide a quantitative study of the thermodynamic factors that effect the electrochemical oxidation. For example, Pickett and Pletcher[3] have developed a three-parameter equation for correlating the one-electron oxidation potential of the

(1) Deakin University.
(2) University of Melbourne.

(3) Pickett, C. J.; Pletcher, D. *J. Organomet. Chem.* **1975**, *102*, 327.

0276-7333/84/2303-0541$01.50/0

$[M(CO)_{6-x}L_x]^{Y+}$ (M = Cr, Mn; L = CNMe) systems with the value of x. Unfortunately the model does not explain differences noted experimentally between isomeric pairs.

Treichel et al.[4] subsequently developed a model that could explain differences in oxidation potentials for isomeric pairs of $[Mn(CO)_n(CNCH_3)_{6-n}]^+$ for n = 2 (cis,trans) and n = 3 (*fac*, *mer*). More recently Bursten[5] extended these theories for low-spin octahedral systems $ML_nL'_{6-n}$ (M = Cr°, Mn^+; L, L′ = different ligands). This model predicts that the $E°$ for systems such as *cis*- and *trans*-$M(CO)_4L'_2$ should be identical, that *fac*-$M(CO)_3L'_3$ should be more difficult to oxidize than *mer*-$M(CO)_3L'_3$, and that in the dicarbonyl complexes $M(CO)_2L'_4$, the cis isomer should be harder to oxidize than the trans isomer.

Theoretical calculations by Mingos[6] led to the conclusion that electronic (as well as steric effects) favor the formation of the trans or *mer* isomer in the 17-electron systems. However, in the 18-electron system steric and electronic effects favor different isomers so that either isomer may be favored depending on the balance between these effects. Consequently oxidation of 18-electron carbonyl compounds might not lead to simple redox couples between isostructural pairs since structural changes may accompany charge transfer. Great care is therefore needed in the interpretation of electrochemical data (e.g., cyclic voltammetry).[7] Work by Chatt et al.[8] and Lloyd et al.[9] illustrated that substituent effects are very important in the electrochemistry of carbonyl compounds.

In summary, consideration of redox potentials requires that the thermodynamic and kinetic influences of geometry and substituent effects be taken into account in both halves of the redox couple.

Previous data on oxidation of $Mo(CO)_3L_3$ are not very extensive.[10-12] For complexes of the type $Mo(CO)_3(L)$ (L = polycyclic tridentate ligand with P, S, or N donors) the stereochemistry of the complex was fixed in the facial form and consequently two quasi-reversible one-electron oxidations were observed.[10] In contrast, for the complexes $Mo(CO)_3(carbene)_2(L)$ (L = monodentate P or N donor) careful work was required to elucidate the structures of the isomeric compounds produced after the one-electron oxidation of 18- electron compounds.[11] In other brief reports polarographic oxidation of $HB(pz)_3Mo(CO)_3^-$ (where $HB(pz)_3^-$ is hydrotris(1-pyrazole)borate) showed that this complex undergoes two discrete one-electron oxidation steps[12a] and oxidation of some facial molydenum tricarbonyl isocyanide and acetonitrile complexes has been reported without a detailed interpretation of the electrode processes being provided.[12b,c]

In the present work we have investigated the one-electron oxidation of the compounds *fac*-$Mo(CO)_3P_3$ (P = $P(OMe)_3$, $P(OMe)_2Ph$, $P(OMe)Ph_2$, PMe_2Ph, $P(OPh)_3$, $P(CH_2Ph)Ph_2$) to study substituent effects and the influence of geometry of the redox couples. To aid the investigation NMR and infrared measurements were utilized.

Recent work from these laboratories on the isoelectronic d^6 $Cr(CO)_3P_3$ complexes (P = mododentate phosphine or phosphite) showed the importance of isomerization, cross redox, and self-exchange reactions.[13]

Experimental Section

Reagents. The phosphorus ligands were obtained commercially and distilled or recrystallized before use except $P(OMe)_2Ph$ and $P(OMe)Ph_2$ which were prepared by the published methods.[14] Molybdenum tricarbonyl cycloheptatriene was prepared by the published method.[15] All solvents were dried over type 4A molecular sieves. Tetrabutylammonium perchlorate was dried under vacuum over P_2O_5. $NOPF_6$ and $NOBF_4$ were commercial samples and were used as supplied.

Preparations. The compounds *fac*-$Mo(CO)_3(P(OMe)_3)_3$,[16] *fac*-$Mo(CO)_3(P(OMe)_2Ph)_3$,[17] *fac*-$Mo(CO)_3(P(OMe)Ph_2)_3$,[17] *fac*-$Mo(CO)_3(PMe_2Ph)_3$,[17] *mer*-$Mo(CO)_3(PMe_2Ph)_3$,[17] *fac*-$Mo(CO)_3(P(OPh)_3)_3$,[18] *mer*-$Mo(CO)_3(P(OPh)_3)_3$,[19] and *fac*-$Mo(CO)_3(P(CH_2Ph)Ph_2)_3$[19] were prepared by the published methods.

Instrumentation. (a) Electrochemical. All voltammograms and polarograms were recorded in dichloromethane (0.1 M Bu_4NClO_4) by using a Model 174A E.G. and G PAR electrochemistry system. A three-electrode system was used. Controlled drop times of 0.5, 1.0, and 2.0 s were used in the polarographic measurements. In cyclic voltammetry the working electrode was a hanging mercury drop or a platinum disk. The reference electrode was Ag/AgCl (CH_2Cl_2; saturated LiCl) separated from the test solution by a salt bridge containing 0.1 M tetrabutylammonium perchlorate in dichloromethane. The third or auxiliary electrode was a platinum wire. For variable-temperature cyclic voltammetry the temperature was regulated by using a dry ice/ethanol bath with varying dry ice/ethanol proportions. The temperature was monitored with a thermocouple.

(b) Nuclear Magnetic Resonance. All NMR spectra were recorded on a JEOL FX-100 spectrometer in $CDCl_3$ solution. The $^{31}P\{^1H\}$ NMR spectra were recorded at 40.32 MHz by using 85% H_3PO_4 as external reference. The $^{13}C\{^1H\}$ NMR spectra were recorded at 25.47 MHz by using tetramethylsilane as internal reference. Chromium tris(acetylacetonate) was added to reduce the relaxation time of the ^{13}C nuclei associated with the carbonyl group. The $^{95}Mo\{^1H\}$ NMR spectra were measured at 6.49 MHz relative an external reference of Na_2MoO_4 buffered at pH 11.

(c) Infrared Spectra. The infrared spectra were recorded on a JASCO A-302 spectrometer calibrated against polystyrene (1601 cm^{-1}).

The infrared spectra of *mer*-$[Mo(CO)_3P_3]^+$ derivatives were recorded at room temperature on samples prepared by in situ oxidation of *fac*-$Mo(CO)_3P_3$ with $NOBF_4$ in dichloromethane at 0 °C.

Results and Discussion

The $Mo(CO)_3(PMe_2Ph)_3$ System. Generally for $Mo(CO)_3P_3$ only the facial isomer is readily prepared, but for P = PMe_2Ph it is possible to prepared both the meridional and facial isomers. Access to both isomers, in which the 18-electron compounds do not readily interconvert, allowed the processes after oxidation to be readily characterized. Furthermore, both isomers oxidized at a potential suffi-

(4) Treichel, P. M.; Much, H. J.; Bursten, B. E. *Isr. J. Chem.* **1977**, *15*, 253.
(5) Bursten, B. E. *J. Am. Chem. Soc.* **1982**, *104*, 1299.
(6) Mingos, D. M. P. *J. Organomet. Chem.* **1979**, *179*, C29.
(7) Bond, A. M.; Darensbourg, D. J.; Mocellin, E.; Stewart, B. J. *J. Am. Chem. Soc.* **1981**, *103*, 6827.
(8) (a) Crichton, B. A. L.; Dilworth, J. R.; Pickett, C. J.; Chatt, J. *J. Chem. Soc., Dalton Trans.* **1981**, 419. (b) Chatt, J.; Leigh, G. J.; Neukomm, H.; Pickett, C. J.; Stanley, D. R. *Ibid.* **1980**, 121. (c) Butler, G.; Chatt, J.; Leigh, G.; Pickett, C. J. *Ibid.* **1979**, 113.
(9) Lloyd, M. K.; McCleverty, J. A.; Orchard, D. G.; Connor, J. A.; Hall, M. B.; Hillier, I. H.; Jones, E. M.; McEwen, G. K. *J. Chem. Soc., Dalton Trans.* **1973**, 1743.
(10) Fox, M. A.; Campbell, K. A.; Kyba, E. P. *Inorg. Chem.* **1981**, *20*, 4163.
(11) Rieke, R. D.; Kojima, H.; Oefele, K. *Angew. Chem., Int. Ed. Engl.* **1980**, *19*, 538.
(12) (a) Trofimenko, S. *J. Am. Chem. Soc.* **1969**, *91*, 588. (b) Connor, J. A.; Jones, E. M.; McEwan, G. K.; Lloyd, M. K.; McCleverty, J. A. *J. Chem. Soc., Dalton Trans.* **1972**, 1246. (c) Hershberger, J. W.; Klingler, R. J.; Kochi, J. K. *J. Am. Chem. Soc.* **1982**, *104*, 3034.
(13) Bond, A. M.; Carr, S. W.; Colton, R. *Inorg. Chem.*, in press.
(14) Harwood, H. J.; Grisley, D. W., Jr. *J. Am. Chem. Soc.* **1960**, *82*, 423.
(15) Eisch, J. J.; King, R. B., Eds. "Organometallic Syntheses"; Academic Press: New York, 1964; Vol. 1, p 125.
(16) Pidcock, A.; Taylor, B. W. *J. Chem. Soc.* **1967**, 877.
(17) Jenkins, J. M.; Moss, J. R.; Shaw, B. L. *J. Chem. Soc.* **1969**, 2796.
(18) Verkade, J. G.; McCarley, R. E.; Hendricker, D. G.; King, R. W. *Inorg. Chem.* **1965**, *4*, 228.
(19) Magee, T. A.; Matthews, C. N.; Wang, T. S.; Wotiz, J. H. *J. Am. Chem. Soc.* **1961**, *83*, 3200.

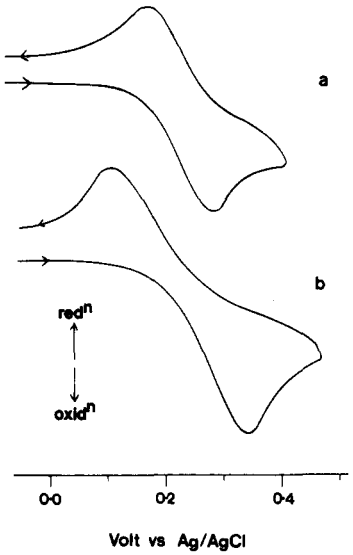

Figure 1. Cyclic voltammogram for the oxidation of a 10^{-3} M solution of *mer*-$Mo(CO)_3(PMe_2Ph)_3$ in dichloromethane (0.1 M Bu_4NClO_4) at 20 °C at 200 mV/s: (a) at a hanging drop mercury electrode; (b) at a platinum electrode.

ciently negative to allow the processes to be studied at both mercury and platinum electrodes.

(i) Electrochemical Oxidation of *mer*-$Mo(CO)_3(PMe_2Ph)_3$. The dc polarogram for oxidation of *mer*-$Mo(CO)_3(PMe_2Ph)_3$ (10^{-3} M) gave one well-defined wave with an $E_{1/2}$ value of 0.215 (±0.005) V vs. Ag/AgCl in CH_2Cl_2 (0.1 M $Bu_4N\ ClO_4$) at 20 °C and a value for $E_{3/4} - E_{1/4}$ of −55 (±1) mV over the drop time range of 0.5–2.0 s. $E_{1/2}$, therefore, closely approximated the standard redox potential $E°$. These data were consistent with a reversible one-electron oxidation. Additionally, the limiting current per unit concentration was similar to that observed for the known one-electron oxidation[13] shown in eq 1. Figure 1a

$$mer\text{-}Cr(CO)_3P_3 \rightleftharpoons mer\text{-}[Cr(CO)_3P_3]^+ + e^- \quad (1)$$

shows the oxidative cyclic voltammogram of *mer*-$Mo(CO)_3(PMe_2Ph)_3$ at a hanging drop mercury electrode at a scan rate of 200 mV/s. A peak to peak separation of 100 mV was observed, and in this time scale the process appeared to be a quasi-reversible one-electron oxidation without any chemical reactions. The calculated $E°$ value of 0.225 (±0.010) V at 20 °C was close to that obtained from polarographic data. (Calculation of $E°$ was based on digital simulation using the method of Feldberg,[20] assuming equal diffusion coefficients for reduced and oxidized species and a charge-transfer coefficient of 0.5). Figure 1b shows the cyclic voltammogram of *mer*-$Mo(CO)_3(PMe_2Ph)_3$ at platinum at a scan rate of 200 mV/s. The peak to peak separation of 230 mV was much larger than that observed at mercury electrodes, indicating that the rate of electron transfer was slower at Pt. However, the calculated $E°$ value of 0.225 (±0.010) V was in excellent agreement with the value observed at the mercury electrode, indicating that the electrode played no role in the chemistry of the redox process. Thus the redox process can be assigned as eq 2. At platinum, a second chemically

$$mer\text{-}Mo(CO)_3(PMe_2Ph)_3 \rightleftharpoons mer\text{-}[Mo(CO)_3(PMe_2Ph)_3{}^+]^+ + e^- \quad (2)$$

irreversible one-electron oxidation with a peak potential of approximately 1.0 V was observed which was assigned

(20) Feldberg, S. W. In "Electroanalytical Chemistry" Bard, A. J., Ed.; Marcel Dekker: New York, 1969; Vol. 3, pp 199–296.

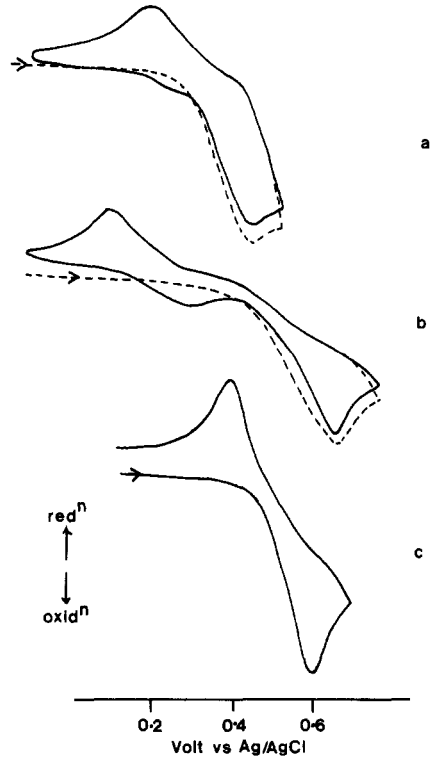

Figure 2. Cyclic voltammograms for the oxidation of a 10^{-3} M solution of *fac*-$Mo(CO)_3(PMe_2Ph)_3$ in dichloromethane (0.1 M Bu_4NClO_4): (a) at 20 °C at a hanging drop mercury electrode (the first oxidation scan is dotted for clarity; scan rate = 200 mV/s); (b) at 20 °C at a platinum electrode (scan rate = 200 mV/s); (c) at −55 °C at a platinum electrode (scan rate 100 V/s). Current axis is not to scale.

to the process shown in eq 3. This second irreversible process will not be discussed further.

$$mer\text{-}[Mo(CO)_3(PMe_2Ph)_3]^+ \rightleftharpoons mer\text{-}[Mo(CO)_3(PMe_2Ph)_3]^{2+} + e^- \quad (3)$$
$$\downarrow$$
products

(ii) Electrochemical Oxidation of *fac*-$Mo(CO)_3(PMe_2Ph)_3$. The dc polarogram for the oxidation of *fac*-$Mo(CO)_3(PMe_2Ph)_3$ (10^{-3} M solution in CH_2Cl_2) occurred near the mercury oxidation limit. The wave exhibited a pronounced maximum for all drop times over the range 0.5–2.0 s. The origin of the maxima is unknown. However, the limiting current per unit concentration (error ±10%) was the same as observed for the oxidation of *mer*-$Mo(CO)_3(PMe_2Ph)_3$ for the same drop time which implied that this process was also a one-electron oxidation. At a drop time of 2 s, $E_{1/2}$ was 0.35 ± 0.02 V with $E_{3/4} - E_{1/4}$ equal to −50 ± 5 mV. As the drop time was decreased, $E_{1/2}$ became more positive and $E_{3/4} - E_{1/4}$ approached the Nernstian value. Data were consistent with a reversible charge transfer followed by chemical reaction.

From the drop time dependence the $E°$ value for the redox couple shown in eq 4 was calculated to be approx-

$$fac\text{-}Mo(CO)_3(PMe_2Ph)_3 \rightleftharpoons fac\text{-}[Mo(CO)_3(PMe_2Ph)_3]^+ + e^- \quad (4)$$

imately 0.40 V. The chemical reaction associated with charge transfer was presumed at this stage to be the isomerization reaction (5).

$$fac\text{-}[Mo(CO)_3(PMe_2Ph)_3]^+ \rightarrow mer\text{-}[Mo(CO)_3(PMe_2Ph)_3]^+ \quad (5)$$

The cyclic voltammogram at a hanging drop mercury electrode at a scan rate of 200 mV/s is shown in Figure 2a. On the initial oxidation scan only one peak is observed at 0.43 V. On reversing the scan direction a weak reduction peak at ~0.39 V and a much better defined reduction process at 0.18 V were observed. On second and subsequent scans an oxidation response at 0.24 V was observed in addition to the features described above. The electrochemical processes described above can be summarized as shown in eq 6–8. The assignment of the $mer^{+/0}$ couple

$$fac\text{-}Mo(CO)_3(PMe_2Ph)_3 \rightleftharpoons fac\text{-}[Mo(CO)_3(PMe_2Ph)_3]^+ + e^- \quad (6)$$

$$fac\text{-}[Mo(CO)_3(PMe_2Ph)_3]^+ \rightarrow mer\text{-}[Mo(CO)_3(PMe_2Ph)_3]^+ \quad (7)$$

$$mer\text{-}[Mo(CO)_3(PMe_2Ph)_3]^+ + e^- \rightleftharpoons mer\text{-}Mo(CO)_3(PMe_2Ph)_3 \quad (8)$$

was made by comparison with the waves observed directly for *mer*-$Mo(CO)_3(PMe_2Ph)_3$. Repetitive scanning increased the ratio of the oxidation peak height of mer^0 relative to fac^0. Concentration dependence studies indicated that a nonunity reaction order was present. The above observations were best explained by the cross redox reaction (9). Cyclic voltammograms were recorded at

$$fac\text{-}[Mo(CO)_3(PMe_2Ph)_3]^+ + mer\text{-}Mo(CO)_3(PMe_2Ph)_3 \rightleftharpoons fac\text{-}Mo(CO)_3(PMe_2Ph)_3 + mer\text{-}[Mo(CO)_3(PMe_2Ph)_3]^+ \quad (9)$$

platinum electrodes over a wide range of scan rates, and the results confirmed that the electrode processes observed at platinum were the same as those at mercury except that electron transfer was much slower at platinum. As an example, the cyclic voltammogram at room temperature at a scan rate of 200 mV/s is shown in Figure 2b. At this scan rate and temperature there was no reversibility in the $fac^{+/0}$ couple. At very fast scan rates (e.g., 10 V/s) some reversibility was noted for the $fac^{+/0}$ couple and concomitantly the current due to the $mer^{+/0}$ couple decreased. At scan rates of 1 V/s the appearance of the $mer^{+/0}$ couple observed on second and subsequent scans approached that expected for a reversible couple, i.e., i_p^{ox}/i_p^{red} approached unity (i_p is the peak height). This provided further evidence that the cross redox reaction (eq 9) was operative. At slower scan rates (e.g., 50 mV/s) the $mer^+ \rightarrow mer^0$ reduction peak was still very well-defined although i_p^{ox}/i_p^{red} was very much less than unity. After a few electrochemical experiments small amounts of *mer*-$Mo(CO)_3(PMe_2Ph)_3$ could be detected in the bulk solution by cyclic voltammetry. Repeated experiments resulted in the gradual decrease in the peak height for *fac* oxidation and a corresponding increase for *mer* oxidation. All these data are consistent with the isomerization process (10) and the cross redox reaction (eq 9) being important.

$$fac\text{-}[Mo(CO)_3(PMe_2Ph)_3]^+ \rightarrow mer\text{-}[Mo(CO)_3(PMe_2Ph)_3]^+ \quad (10)$$

The cyclic voltammetry was simplified substantially on lowering the temperature. Figure 2c shows the cyclic voltammogram at platinum for *fac*-$Mo(CO)_3(PMe_2Ph)_3$ at −55 °C. At this temperature the simple quasi-reversible couple shown in eq 11 was observed. No evidence for the

$$fac\text{-}Mo(CO)_3(PMe_2Ph)_3 \rightleftharpoons fac\text{-}[Mo(CO)_3(PMe_2Ph)_3]^+ + e^- \quad (11)$$

generation of mer^0 or mer^+ could be found on the second scan. The calculated E° value was 0.49 V at −55 °C compared with 0.23 V at −55 °C for *mer*-$Mo(CO)_3(PMe_2Ph)_3$.

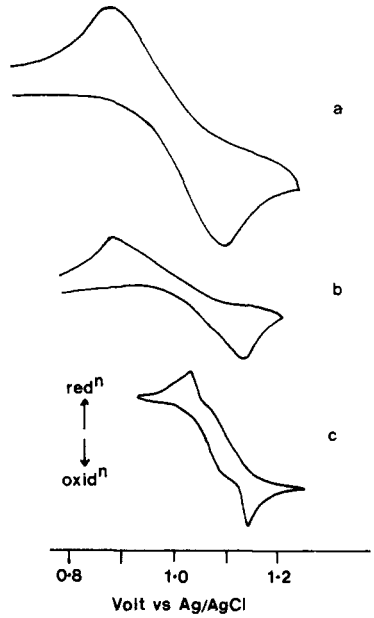

Figure 3. Cyclic voltammograms in dichloromethane solution (0.1 M Bu_4NClO_4) at a platinum electrode for the oxidation of 10^{-3} M solutions of (a) *mer*-$Mo(CO)_3(P(OPh)_3)_3$ at 20 °C (scan rate = 100 mV/s), (b) *fac*-$Mo(CO)_3(P(OPh)_3)_3$ at 20 °C (scan rate = 100 mV/s) and (c) *fac*-$Mo(CO)_3(P(OPh)_3)_3$ at −55 °C (scan rate = 10 mV/s) under a steady-state conditions. Current axis is not to scale.

(iii) Chemical Oxidation of *mer*- and *fac*-$Mo(CO)_3(PMe_2Ph)_3$. Addition of solid $NOBF_4$ to a 10^{-3} M solution of *fac*- or *mer*-$Mo(CO)_3(PMe_2Ph)_3$ at 20 °C caused the disappearance of the polarographic oxidation wave. In its place a polarographic reduction wave with an $E_{1/2}$ of 0.21 V was observed. The $E_{1/2}$ value of the new wave was coincident with that observed for the oxidation of *mer*-$Mo(CO)_3(PMe_2Ph)_3$. The limiting current, however, for the reduction process was much smaller than for the initial oxidation, and furthermore the reduction current decayed as a function of time. This indicated that *mer*-$[Mo(CO)_3(PMe_2Ph)_3]^+$ was not stable at room temperature. Infrared studies that confirmed the above structural assignment (see later) also indicated the instability of *mer*-$[Mo(CO)_3(PMe_2Ph)_3]^+$ at room temperature.

The $Mo(CO)_3(P(OPh)_3)$ System. For $Mo(CO)_3(P(OPh)_3)$ both isomers were again available, and therefore the electrochemistry will be considered in detail. Both isomers of $Mo(CO)_3(P(OPh)_3)$ were oxidized at a potential too positive to be studied at mercury; consequently only data at a platinum electrode are available.

(i) Electrochemical Oxidation of *mer*-$Mo(CO)_3(P(OPh)_3)_3$. Figure 3a shows cyclic voltammogram of *mer*-$Mo(CO)_3(P(OPh)_3)_3$ at a scan rate of 200 mV/s. Digital simulation of the curve over scan rates of 50–500 mV/s at 20 °C using the quasi-reversible model of Feldberg[20] gave an E° value of 0.980 V which was independent of scan rate. At −55 °C the E° value was calculated to be 1.060 ± 0.05 V. The data fitted the quasi-reversible model of electron transfer. The electrode process can thus be written as eq 12.

$$mer\text{-}Mo(CO)_3(P(OPh)_3)_3 \rightleftharpoons mer\text{-}[Mo(CO)_3(P(OPh)_3)_3]^+ + e^- \quad (12)$$

(ii) Electrochemical Oxidation of *fac*-$Mo(CO)_3(P(OPh)_3)_3$. Under some conditions the cyclic voltammograms at a platinum electrode of *fac*-$Mo(CO)_3P(OPh)_3$ superficially appeared to be quasi-reversible one-electron oxidations. For example, Figure 3b shows the cyclic

Table I. The Electrochemical Data and ln K for the Equilibrium

$$fac^+ + mer^0 \overset{K}{\rightleftharpoons} fac^0 + mer^+$$

for $M(CO)_3P_3$ (M = Mo, Cr) Systems at −55 °C (10^{-3} M Concentration)

	compd	M(O) → M(I) $E^\circ(fac^{+/0})$, V	M(O) → M(I) $E^\circ(mer^{+/0})$, V	M(O) → M(I) ΔE°, V	ln K	M(I) → M(II) E_p^{ox}, V
1	$Mo(CO)_3(PMe_2Ph)_3$	0.49	0.23	0.26	13.85	1.0
2	$Mo(CO)_3(P(OPh)_3)_3$	1.10	1.06	0.04	2.13	*b*
3	$Mo(CO)_3(P(OMe)_3)_3$	0.83	0.66	0.17	9.06	1.5
4	$Mo(CO)_3(P(OMe)_2Ph)_3$	0.78	0.54	0.24	12.79	1.4
5	$Mo(CO)_3(P(OMe)Ph_2)_3$	0.61	0.47	0.14	7.46	1.2
6	$Mo(CO)_3(PPh_2(CH_2Ph))_3$	0.93	0.85	0.08	4.26	*b*
7	$Cr(CO)_3(PMe_2Ph)_3$ [c]	0.22	−0.05	0.27	14.38	1.1
8	$Cr(CO)_3(P(OMe)_3)_3$ [c]	0.53	0.38	0.15	8.00	1.5

[a] All potentials vs. Ag/AgCl. [b] Not observed prior to solvent limit. [c] Data from ref 13.

voltammogram at 20 °C (scan rate = 100 mV/s). The shape of the wave indicated that slow electron transfer was occurring and the peak to peak separation was similar to that observed for *mer*-$Mo(CO)_3(P(OPh)_3)_3$. However, theoretical treatment of the data in terms of the quasi-reversible one-electron oxidation shown in eq 13 indicated

$$fac\text{-}Mo(CO)_3(P(OPh)_3)_3 \rightleftharpoons fac\text{-}[Mo(CO)_3(P(OPh)_3)_3]^+ + e^- \quad (13)$$

that the experimental data did not fit this model at all scan rates. At slower scan rates the data departed substantially from the quasi-reversible model. Repeated cyclic voltammetric scans at −55 °C and very slow scan rates were required to reveal the presence of two overlapping redox couples (Figure 3c). Oxidation of the facial isomer is in fact more positive than for the meridional form, although the E°'s for the $fac^{+/0}$ and $mer^{+/0}$ are very similar. Problems associated with this kind of system have been dealt with elsewhere.[21] The full reaction scheme is shown in eq 14, where (k_s) represents the heterogenous charge-

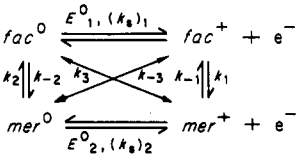

(14)

transfer rate constant 1 or 2, k_n and k_{-n} are homogeneous rate constants for isomerization steps, and × represents the cross redox reaction $fac^+ + mer^0$ $(k_3) \rightleftharpoons fac^0 + mer^+$ (k_{-3}) with k_3 and k_{-3} being second order homogeneous rate constants.

These data could easily be misinterpreted as either eq 15 or eq 16. Theoretical examination of this square re-

$$fac\text{-}Mo(CO)_3(P(OPh)_3)_3 \overset{\text{slow electron transfer}}{\rightleftharpoons} fac\text{-}[Mo(CO)_3(P(OPh)_3)_3]^+ + e^- \quad (15)$$

$$fac\text{-}Mo(CO)_3(P(OPh)_3)_3 \overset{\text{slow electron transfer}}{\rightleftharpoons} mer\text{-}[Mo(CO)_3(P(OPh)_3)_3]^+ + e^- \quad (16)$$

action scheme (eq 14) for the limiting case where the charge-transfer steps for both couples are reversible, i.e., $(k_s)_1$ and $(k_s)_2$ very large, have been undertaken.[22] In the present case cyclic voltammetry of the pure *mer*-$Mo(CO)_3(P(OPh)_3)_3$ showed that these assumptions were not strictly valid and that both steps were only quasi-reversible. At low temperatures and low scan rates, assuming the cross redox reaction was inoperative on the electrochemical time scale and that charge transfer was reversible, the calculated E° for processes 17 and 18 are as shown.

$$fac\text{-}Mo(CO)_3(P(OPh)_3)_3 \overset{E^\circ = 1.10\text{ V}}{\rightleftharpoons} fac\text{-}[Mo(CO)_3(P(OPh)_3)_3]^+ + e^- \quad (17)$$

$$mer\text{-}Mo(CO)_3(P(OPh)_3)_3 \overset{E^\circ = 1.06\text{ V}}{\rightleftharpoons} mer\text{-}Mo(CO)_3(P(OPh)_3)_3^+ + e^- \quad (18)$$

The major difference between the $Mo(CO)_3(P(OPh)_3)_3$ system and the $Mo(CO)_3(PMe_2Ph)_3$ system was that the E°'s for the $fac^{+/0}$ and $mer^{+/0}$ couples were much more widely separated in the PMe_2Ph system and thus the system was easier to study. This meant that the equilibrium constant for the cross redox reaction (19) was much

$$fac^+ + mer^0 \overset{K}{\rightleftharpoons} fac^0 + mer^+ \quad (19)$$

larger for the $Mo(CO)_3(PMe_2Ph)_3$ system than for the $Mo(CO)_3(P(OPh)_3)_3$ system. Obviously this equilibrium constant has a large substituent effect.

(iii) Chemical Oxidation of *mer*- and *fac*-$Mo(CO)_3(P(OPh)_3)_3$. As for *fac*/*mer*-$Mo(CO)_3(PMe_2Ph)_3$ the $NOBF_4$ oxidation of *fac*- or *mer*-$Mo(CO)_3(P(OPh)_3)_3$ produced *mer*-$Mo(CO)_3(P(OPh)_3)_3]^+$ which was characterized by infrared spectroscopy (see later). The molybdenum(I) compound was observed to be unstable at room temperature as its polarographic response decrease to zero over a period of minutes, and thus this cation could not be isolated.

Electrochemical Oxidation of the Other $Mo(CO)_3P_3$ Systems. For the compounds *fac*-$Mo(CO)_3P_3$ (P = P(OMe)$_3$, P(OMe)$_2$Ph, P(OMe)Ph$_2$, PPh$_2$(CH$_2$Ph)) only the facial isomers are readily available. The cyclic voltammograms are always very scan and temperature dependent and on no occasion did they fit the quasi-reversible one-electron oxidation model, although under some circumstances they superficially resembled quasi-reversible couples. With use of the detailed studies described above for the $Mo(CO)_3(PMe_2Ph)_3$ and $Mo(CO)_3(P(OPh)_3)_3$ systems the electrode processes observed for these compounds could be described by the square reaction scheme (eq 14). Table I summerizes the calculated E° values.

The cyclic voltammogram of *fac*-$Mo(CO)_3(PPh_2(CH_2Ph))_3$ at 20 °C is shown in Figure 4 (scan rate = 200 mV/s). It has the form of an almost irreversible oxidation. At faster scan rates the degree of reversibility increased while at slower scan rates the degree of reversibility decreased. At −55 °C the cyclic voltammograms resemble those obtained for the other $Mo(CO)_3P_3$ systems with the total oxidation current being approximately equal to the total reduction current. Thus the reaction scheme for *fac*-$Mo(CO)_3(PPh_2(CH_2Ph))_3$ at room temperature in-

(21) See ref 7.
(22) Bond, A. M.; Oldham, K. B. *J. Phys. Chem.* **1983**, *87*, 2492.

Table II. The ^{13}C, ^{31}P, and ^{95}Mo NMR Parameters for the Compounds $Mo(CO)_3P_3$ in $CDCl_3$ at 25 °C

compd	$\delta(^{13}C)^a$	$\delta(^{31}P)^a$	$^2J_{P,P}$, ^{b} Hz	$\delta(^{95}Mo)^c$	$^1J_{Mo-P}$, ^{b} Hz
mer-$Mo(CO)_3(PMe_2Ph)_3$	221.5 (1)	8.1 (2)	22.5		
	214.7 (2)	−3.3 (1)			
mer-$Mo(CO)_3(P(OPh)_3)_3$	211.4 (1)	62.9 (2)	47.5		
	207.5 (2)	55.9 (1)			
fac-$Mo(CO)_3(PMe_2Ph)_3$	219.4	5.3		−1486	126.9
fac-$Mo(CO)_3(P(OPh)_3)_3$	211.8	144.6		−1673	239.0
fac-$Mo(CO)_3(P(OMe)_3)_3$	215.2	167.1		−1758	214.8
fac-$Mo(CO)_3(P(OMe)_2Ph)_3$	216.4	182.0		−1611	185.4
fac-$Mo(CO)_3(P(OMe)Ph_2)_3$	218.0	142.7		−1454	156.4
fac-$Mo(CO)_3(PPh_2(CH_2Ph))_3$	215.5	29.0			18.1

^{a} Error ±0.1 ppm. ^{b} Error ±0.4 Hz. ^{c} Error ±1 ppm.

Table III. The Infrared Carbonyl Stretching Frequencies of $Mo(CO)_3P_3$ and $[Mo(CO)_3P_3]^+$ in Dichloromethane at 22 °C

compd	ν_{CO}, ^{b} cm^{-1}				
mer-$Mo(CO)_3(PMe_2Ph)_3$	1960 w		1890 w		1847 s
fac-$Mo(CO)_3(PMe_2Ph)_3$		1935 s		1830 s	
mer-$Mo(CO)_3(P(OPh)_3)_3$	2040 m		1910 s		1890 sh
fac-$Mo(CO)_3(P(OPh)_3)_3$		1991 s		1929 s	
fac-$Mo(CO)_3(P(OMe)_3)_3$		1970 s		1880 s	
fac-$Mo(CO)_3(P(OMe)_2Ph)_3$		1963 s		1874 s	
fac-$Mo(CO)_3(P(OMe)Ph_2)_3$		1955 s		1868 s	
fac-$Mo(CO)_3(PPh_2(CH_2Ph))_3$		1910 s		1875 m	
mer-$[Mo(CO)_3(PMe_2Ph)_3]^+$	2060 m		2030 sh		1972 s
mer-$[Mo(CO)_3(P(OPh)_3)_3]^+$	2150 w		2050 s		1970 m
mer-$[Mo(CO)_3P(OMe)_3)_3]^+$	2120 w		2070 m		2000 s
mer-$[Mo(CO)_3(P(OMe)_2Ph)_3]^+$	2102 w		2052 m		1997 s
mer-$[Mo(CO)_3(P(OMe)Ph_2)_3]^+$	2112 w		2052 m		1995 s
mer-$[Mo(CO)_3(PPh_2(CH_2Ph))_3]^+$			*a*		

^{a} Too unstable to be observed (see text). ^{b} s = strong, m = medium, w = weak, sh = shoulder.

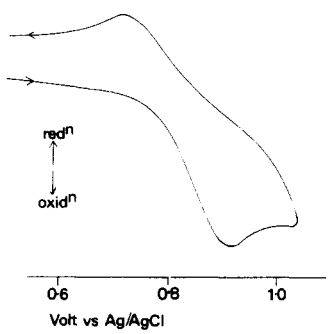

Figure 4. Cyclic voltammogram for the oxidation of a 10^{-3} M solution of *fac*-$Mo(CO)_3(PPh_2(CH_2Ph))_3$ in dichloromethane (0.1 M Bu_4NClO_4) at 20 °C at a platinum electrode (scan rate 200 mV/s).

cluded processes 20–23 with the processes described in eq 22 and 23 being important. A −55 °C eq 22 and 23 ceased to operate, and the square reaction scheme (eq 14) explained the electrochemical behavior.

$$fac\text{-}Mo(CO)_3(PPh_2(CH_2Ph))_3 \rightleftharpoons fac\text{-}[Mo(CO)_3(PPh_2(CH_2Ph))_3]^+ + e^- \quad (20)$$

$$fac\text{-}[Mo(CO)_3(PPh_2(CH_2Ph))_3]^+ \rightleftharpoons mer\text{-}[Mo(CO)_3(PPh_2(CH_2Ph))_3]^+ \quad (21)$$

$$fac\text{-}[Mo(CO)_3(PPh_2(CH_2Ph))_3]^+ \rightarrow \text{products} \quad (22)$$

$$mer\text{-}[Mo(CO)_3(PPh_2(CH_2Ph))_3]^+ \rightarrow \text{products} \quad (23)$$

Infrared spectra of the products formed in eq 22 and 23 showed that they do not contain carbon monoxide.

NMR Spectra of *fac*- and *mer*-$Mo(CO)_3P_3$. The ^{31}P, ^{13}C, and ^{95}Mo NMR spectra data are given in Table II. The $^{31}P\{^1H\}$ NMR spectra of the compounds *mer*-$Mo(CO)_3P_3$ showed second-order effects but were readily solved as A_2B-type spectra. The $^{13}C\{^1H\}$ spectra, in the carbonyl region, consisted of two multiplets, one at lower frequency of intensity 2 and one at higher frequency of intensity 1. For *fac*-$Mo(CO)_3P_3$ the $^{31}P\{^1H\}$ NMR spectra showed a singlet, and in some cases six equally spaced satillites due to coupling to ^{95}Mo ($I = {}^5/_2$, 15.5%) were observed. The $^{13}C\{^1H\}$ NMR spectra in the carbonyl region each gave a multiplet due to coupling to the magnetically inequivalent phosphorus nuclei. The ^{95}Mo NMR spectra could only be obtained for the more soluble facial compounds and consisted of a quartet due to coupling to three equivalent phosphorus nuclei. For $Mo(CO)_3(PMe_2Ph)_3$ and $Mo(CO)_3(P(OPh)_3)_3$ the ^{31}P NMR spectrum of a mixture *fac* and *mer* isomers showed separate signals at room temperature. All the these data show that *fac*^{0} and *mer*^{0} isomers are rigid on the NMR time scale.

Infrared Spectra of $[Mo(CO)_3P_3]^+$ Compounds. The infrared spectra of the compounds $[Mo(CO)_3P_3]^+$, prepared by in situ $NOBF_4$ oxidation in CH_2Cl_2, showed three bands in the carbonyl region, one of which was weak and the other two were much stronger in intensity (Table III). These data were consistent with the formation of the *mer* isomer (C_{2v} symmetry).[23] The carbonyl infrared stretching frequencies of the Mo(I) compounds were moved to higher frequencies relative to the analogous Mo(0) compounds. This was consistent with the molybdenum(I) center being less able to π back-bond to the carbonyl groups.

The lack of stability of the 17-electron molybdenum(I) tricarbonyl compounds observed in the polarographic experiments was confirmed from infrared spectra in the carbonyl region. The absorptions due to the carbonyl groups of freshly prepared solutions of *mer*-$[Mo(CO)_3P_3]^+$ in dichloromethane disappeared in about 10 min at room temperature. In the case of $Mo(CO)_3(PPh_2(CH_2Ph))_3$ no spectrum attributable to the 17-electron Mo(I) complex was observed. This observation was consistent with the lower stability of this compound on the electrochemical time scale.

(23) Braterman, P. S. "Metal Carbonyl Spectra"; Academic Press: London, 1975.

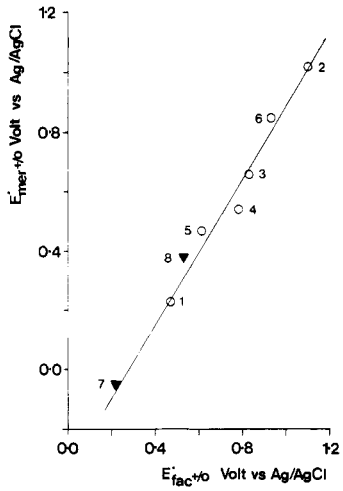

Figure 5. Plot of $E^{\circ}(mer^{+/0})$ against $E(fac^{+/0})$ (both V vs. Ag/AgCl). Processes are defined as in text. Circles (○) represents points for $[Mo(CO)_3P]^{+/0}$ couples, and triangles (▼) represent $[Cr(CO)_3P_3]^{+/0}$ couples. compounds are identified in Table I. Least-squares fit: slope = 1.2 (±0.07); intercept = −0.31 (±0.5) V; correlation coefficient = 0.98.

General Trends in $Mo(CO)_3P_3$ Electrochemistry. The E° values of the $Mo(CO)_3P_3$ systems occurred over the large potential range, 0.23–1.10 V (Table I), which indicated that a large substituent effect is operative in these compounds. For a particular phosphorus ligand the E° values of the $fac^{+/0}$ couple occurred at a more positive potential than the $mer^{+/0}$ couple which confirms the prediction of the model proposed by Bursten.[5] This three-parameter model predicts that a linear relationship should exist between $E^{\circ}(fac^{+/0})$ and $E^{\circ}(mer^{+/0})$. For the $Mo(CO)_3P_3$ compounds an approximately linear correlation was observed (Figure 5). Interestingly, the E° values of the $fac^{+/0}$ and $mer^{+/0}$ were closer together for the harder to oxidize compounds.

The value of ln K (eq 19), the equilibrium constant for the cross redox reaction, covered a considerable range (Table I). The range of values of ln K suggests that the importance of the cross redox reaction in the electrochemistry of the molybdenum tricarbonyl compounds is determined to a large extent by the nature of the phosphorus ligands.

Comparison of Electrochemical Data of $Mo(CO)_3P_3$ and $Cr(CO)_3P_3$. The electrochemical data for the isostructural chromium systems $Cr(CO)_3P_3$ (P = PMe_2Ph, $P(OMe)_3$) are given in Table I, and although limited to two compounds, several conclusions can be drawn.

For $[Mo(CO)_3P_3]^+$ and $[Cr(CO)_3P_3]^+$ the mer^+ isomer is strongly favored and intramolecular isomerization between fac^+ and mer^+ was fast whereas in the 18-electron configuration either isomer may be favored and intramolecular isomerization between *fac* and *mer* was slow. These observations essentially agree with the predictions derived from extended Hückel calculations by Mingos.[6] For the same phosphorus ligand, the $Cr(CO)_3P_3$ compounds were easier to oxidize than the corresponding $Mo(CO)_3P_3$ compounds, and for both molybdenum and chromium complexes the E° values for P = PMe_2Ph occurred at lower potential than for P = $P(OMe)_3$ which suggested a similar substituent effect operates for the two metals, as has been observed previously.[24]

The largest difference in the properties of the $Mo(CO)_3P_3$ system and $Cr(CO)_3P_3$ was the greater kinetic lability of the molybdenum systems relative to the chromium systems as indicated by the following evidence. The chromium(I) compounds were readily isolated as solids and only slowly decomposed in solution whereas the molybdenum(I) compounds rapidly decomposed in solution and could not be isolated in the solid state. On the electrochemical time scale the rate of $fac^+ \rightarrow mer^+$ isomerization was observed to be much faster for the molybdenum compounds relative to their chromium analogues.

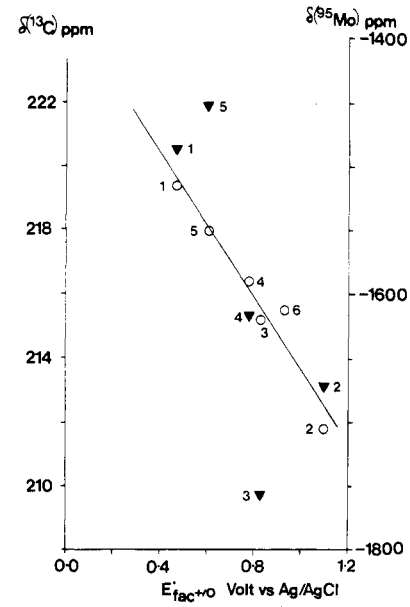

Figure 6. Plots of $\delta(^{13}C)$ of the carbonyl ligands (left-hand scale, ○) and $\delta(^{95}Mo)$ (right-hand scale, ▼) of *fac*-$Mo(CO)_3P_3$ against $E^{\circ}(fac^{+/0})$ (V (vs. Ag/AgCl)). Compounds are identified in Table I. Least-squares fit for $\delta(^{13}C)$ vs. $E^{\circ}(fac^{+/0})$: slope = 1.1 (±0.1) ppm V^{-1}; intercepts = 225 (±) ppm; correlation coefficient = 0.97. Least-squares fit for $\delta(^{95}Mo)$ vs. $E^{\circ}(fac^{+/0})$: slope = −4 (±2) ppm V^{-1}; intercept −1.3 (±0.2) × 10^3 ppm; correlation coefficient = 0.71.

Correlation of NMR Data with Electrochemical Data. Figure 6 shows a plot of $\delta(^{13}C)$ of the equivalent carbonyl ligands of *fac*-$Mo(CO)_3P_3$ against $E^{\circ}(fac^{+/0})$. Previous studies[25] on $Cr(CO)_5L$ (L = P, N, CO, or halogen donor) have shown that reasonable correlations between E° and $\delta(^{13}C)$ exist because changes in E° and $\delta(^{13}C)$ arise from electronic effects only. Structural change between the 18- or 17-electron systems or steric interactions could cause nonlinear relationships. Thus, in the case of *fac*-$Mo(CO)_3P_3$ the observed correlation showed that both ($E^{\circ}(fac^{+/0})$ and $\delta(^{13}C)$ both arise from electronic effects as in the pentacarbonyl compounds. In both series of compounds the gradient was negative and was of the same order of magnitude. As for the pentacarbonyl compounds no statistically significant correlations were observed between $E^{\circ}(fac^{+/0})$ and $\delta(^{31}P)$ or $\Delta(\delta(^{31}P))$ (where $\Delta(\delta(^{31}P))$ = δ(P(complex)) − δ(P(free ligand))).

Figure 6 also shows a plot of $\delta(^{95}Mo)$ against $E^{\circ}(fac^{+/0})$. This was clearly not a straight line although a correlation appears to exist. Although the known data on ^{95}Mo chemical shifts are limited, results suggest that both electronic and steric effects contribute to the shielding.[26] The relative importance of these effects has not been discussed in detail although the poor correlation for the $Mo(CO)_3P_3$ compounds against $E^{\circ}(fac^{+/0})$ at least suggests that in these compounds steric effects may be significant in their effect on the ^{95}Mo chemical shift.

(24) Bond, A. M.; Colton, R.; Jackowski, J. J. *Inorg. Chem.* **1975**, *14*, 274.

(25) Bond, A. M.; Carr, S. W.; Colton, R.; Kelly, D. P. *Inorg. Chem.* **1983**, *22*, 989.

(26) Andrews, G. T.; Colquhoun, I. J.; McFarlane, W.; Grim, S. O. *J. Chem. Soc., Dalton Trans.* **1982**, 2353 and references cited therein.

Registry No. *fac*-$Mo(CO)_3(PMe_2Ph)_3$, 24554-64-1; *fac*-$Mo(CO)_3(PMe_2Ph)_3^+$, 88375-68-2; *mer*-$Mo(CO)_3(PMe_2Ph)_3$, 24554-82-3; *mer*-$Mo(CO)_3(PMe_2Ph)_3^+$, 88326-31-2; *fac*-$Mo(CO)_3(P(OPh)_3)_3$, 41174-20-3; *fac*-$Mo(CO)_3(P(OPh)_3)_3^+$, 88375-69-3; *mer*-$Mo(CO)_3(P(OPh)_3)_3$, 88375-67-1; *mer*-$Mo(CO)_3(P(OPh)_3)_3^+$, 88326-32-3; *fac*-$Mo(CO)_3(P(OMe)_3)_3$, 15631-24-0; *fac*-$Mo(CO)_3(P(OMe)_3)_3^+$, 88375-70-6; *mer*-$Mo(CO)_3(P(OMe)_3)_3$, 15631-23-9; *mer*-$Mo(CO)_3(P(OMe)_3)_3^+$, 88326-33-4; *fac*-$Mo(CO)_3(P(OMe)_2Ph)_3$, 88376-11-8; *fac*-$Mo(CO)_3(P(OMe)_2Ph)_3^+$, 88375-71-7; *mer*-$Mo(CO)_3(P(OMe)_2Ph)_3$, 26133-41-5; *mer*-$Mo(CO)_3(P(OMe)_2Ph)_3^+$, 88326-34-5; *fac*-$Mo(CO)_3(P(OMe)Ph_2)_3$, 88326-29-8; *fac*-$Mo(CO)_3(P(OMe)Ph_2)_3^+$, 88375-72-8; *mer*-$Mo(CO)_3(P(OMe)Ph_2)_3$, 88375-74-0; *mer*-$Mo(CO)_3(P(OMe)Ph_2)_3^+$, 88326-35-6; *fac*-$Mo(CO)_3(PPh_2(CH_2Ph))_3$, 88326-30-1; *fac*-$Mo(CO)_3(PPh_2(CH_2Ph))_3^+$, 88375-73-9; *mer*-$Mo(CO)_3(PPh_2(CH_2Ph))_3$, 88375-75-1; *mer*-$Mo(CO)_3(PPh_2(CH_2Ph))_3^+$, 88326-36-7.

Synthesis of Sulfidoosmium Carbonyl Cluster Compounds by the Photochemical Decomposition of $HOs_3(CO)_{10}(\mu$-SPh) and Its Subsequent Reactions with Selected Small Molecules. Synthesis and Crystal and Molecular Structure of $Os_3(CO)_9(\mu_3$-CO)(μ_3-S)

Richard D. Adams,* István T. Horváth, and Hoon-Sik Kim

Department of Chemistry, Yale University, New Haven, Connecticut 06511

Received November 10, 1983

Under an atmosphere of carbon monoxide, $HOs_3(CO)_{10}(\mu$-SPh) (I) loses benzene when irradiated to form the new cluster compound $Os_3(CO)_9(\mu_3$-CO)(μ_3-S) (II). II was characterized by a single-crystal X-ray diffraction analysis: space group $P\bar{1}$, No. 2, a = 6.912 (2) Å, b = 9.500 (3) Å, c = 13.235 (6) Å, α = 82.63 (3)°, β = 87.43 (3)°, γ = 72.30 (3)°, V = 821.1 (6) Å^3, Z = 2, ρ_{calcd} = 3.57 g/cm^3. The structure was solved by the heavy-atom method and refined (2258 reflections, $F^2 \geq 3.0\sigma(F^2)$) by full-matrix least-squares to the final residuals R_1 = 0.056 and R_2 = 0.069. The molecular structure of II consists of a triangular cluster of three osmium atoms containing a triply bridging sulfido ligand on one threefold face of the cluster and a triply bridging carbonyl ligand on the opposite threefold face. Each osmium atom contains three linear terminal carbonyl ligands. Two Os–Os separations, 2.826 (1) and 2.825 (1) Å, are slightly shorter than the third, 2.840 (1) Å. In the presence of the reagents H_2, H_2S, COS, and CS_2, I loses both benzene and carbon monoxide when irradiated and yields the products $H_2Os_3(CO)_9(\mu_3$-S) (IV), $H_2Os_3(CO)_8(\mu_3$-S)$_2$ (V), $Os_3(CO)_9(\mu_3$-S)$_2$ (VI), and $Os_3(CO)_8CS(\mu_3$-S)$_2$ (VII), respectively. In the absence of a reagent the hexaosmium disulfido cluster, $Os_6(CO)_{17}(\mu_4$-S)$_2$ (III), is formed. Compounds III, IV, and V were also obtained by the photodecarbonylation of II in the presence of the appropriate reagent. It is proposed that an unsaturated intermediate such as $Os_3(CO)_9(\mu_3$-S) is traversed in the photoreactions of both I and II.

Introduction

It has been shown recently that the pyrolysis of $HOs_3(CO)_{10}(\mu$-SPh) (I) at 150 °C proceeds via the elimination of benzene to produce a variety of new sulfidoosmium carbonyl cluster compounds.[1,2] The distribution of the products is greatly affected by the presence of a carbon monoxide atmosphere and varies according to the carbon monoxide pressure.[2] We have now found that benzene elimination from I is also promoted by irradiation with UV light, and the sulfidoosmium intermediate can be trapped by reaction with selected small molecules. In the absence of such reagents, higher nuclearity sulfidoosmium carbonyl clusters are obtained. The details of these reactions are reported here.

Experimental Section

Photolysis experiments were performed by using an external high-pressure mercury lamp on reaction solutions contained in Pyrex glassware. The solvents, hexane and nonane, were stored over 4-Å molecular sieves and were degassed with a dispersed stream of nitrogen gas before use. Infrared spectra were recorded on a Nicolet 5SX FT-IR spectrophotometer. A Bruker HX 270 FT-NMR spectrometer was used to obtain ^{1}H NMR spectra at 270 MHz. GC analyses were performed on a Perkin-Elmer 990 gas chromatograph using 2% OV101 on Chromosorb WHP, 6 ft × 0.125 in. stainless-steel columns. $HOs_3(CO)_{10}(\mu$-SPh) was prepared as described in the literature.[3]

Synthesis. In a typical preparation a solution of 0.100 g of $HOs_3(CO)_{10}(\mu$-SPh) in 100 mL of hexane was photolyzed under a continuous purge with carbon monoxide for 3 h. After removal of solvent in vacuo, the yellow residue was chromotographed on silica TLC plates. Elution with hexane/CH_2Cl_2 (85:15) separated the starting material (0.028 g) from the product $Os_3(CO)_9(\mu_3$-CO)(μ_3-S) (II). Final purification was obtained by crystallization from hexane solvent (yield: 0.036 g, 41%). Reactions with II were performed similarly. Details of the other reactions are summarized in Table I.

Photolysis of I under CO in Sealed Tube. In a sealed tube a solution of 96 mg of I in 10 mL of nonane was photolyzed under carbon monoxide (1 atm) for 4 h. The yellow solution was analyzed by GC for benzene (28%). The solvent was removed in vacuo, and the yellow residue was put on silica TLC plates. Elution with benzene/CH_2Cl_2 (85:15) separated the unreacted

(1) Adams, R. D.; Yang, L. W. *J. Am. Chem. Soc.* **1982**, *104*, 4115.
(2) Adams, R. D.; Horváth, I. T.; Segmüller, B. E.; Yang, L. W. *Organometallics* **1983**, *2*, 1301.
(3) Crooks, G. R.; Johnson, B. F. G.; Lewis, J.; Williams, I. G. *J. Chem. Soc. A* **1969**, 797.

0276-7333/84/2303-0548$01.50/0